1. Study of associated production of vector bosons and b-jets in pp collisions at the LHC [1]

1.1 Introduction

The vector boson production in association with one and two b jets at the CERN Large Hadron Collider is important for many different experimental and theoretical reasons. Bottom quarks have a peculiar signature which allows one to easily identify them thanks to a displaced decay vertex. The associated production with vector bosons is an important backgrounds to VH production with the Higgs boson decaying to b quarks, and many new physics searches. Theoretically, it offers an interesting testing ground for predictions involving heavy quarks.

There are two possible options for the calculation of processes with b-quarks in the final state at hadron colliders. In the four-flavour scheme (4F) b-quarks are not present in the parton density of the incident protons. They can only be generated in the final state and they are usually massive. In the five-flavour scheme (5F) the b-quark mass is considered small with respect to the scale of the process Q and logarithms of the type $log^m \frac{Q^2}{m_b^2}$ are resummed into a b parton density function. The b-quark is therefore massless in this approach, though higher order mass effects can be included in the calculation. A critical review of the different flavour number schemes and of the status of theoretical calculations is available in Ref. [1]. The two approaches give identical results to all orders in perturbation theory, but they can be different at finite order. In the 4F scheme the computation is more complicate, but the full kinematics of the heavy quarks is taken into account. Furthermore it can be easily interfaced to parton showers, even at NLO using the MC@NLO [2] or the Powheg [3] formalisms. On the other hand logarithms in the initial state are not resummed and could lead to large discrepancies in the inclusive quantities like the total cross-section. In the 5F approach, on the opposite, calculations for the inclusive quantities are highly simplified and generally more accurate, but differential distributions and exclusive observables are technically more involved.

The goal of this study is to compare the most recent measurements with the predictions of the state of the art generators using 4F and 5F scheme. The report is organised as follows. In Section 1.2 we provide a short description of the ATLAS and CMS measurements, available in the Rivet framework, for $V + b + X$ and $V + b\bar{b} + X$, where V is a Z or a W boson. In Section 1.3 we describe the generator setups used to obtain the predictions, which are compared to the measurements in Section 1.4 for the Z and 1.5 for the W, before conclusions are drawn in Section 1.6.

1.2 Rivet Routines

Results in this study were produced using three Rivet routines to compare to published ATLAS and CMS data.

- Measurement of differential production cross-sections for a Z boson in association with b-jets in proton-proton collisions at $\sqrt{s} = 7$ TeV with the ATLAS detector [4] (Rivet routine ATLAS_2014_I1306294). A pair of opposite sign charge dressed leptons[2] (i.e. electrons or muons) with $p_T > 20$ GeV and $|\eta| < 2.5$ are required, with a dilepton mass between 76 and 106 GeV. Anti-k$_t$ 0.4 jets are reconstructed from all final state particles, and required to have $p_T >$20 GeV, $|y| < 2.4$ and not overlap with the leptons used to make the Z candidate ($\Delta R(jet, l) > 0.5$). Jets are labelled as b-jets based on matching with $\Delta R < 0.3$ to a weakly decaying b-hadron with $p_T > 5$ GeV.
  Distributions include the p_T and rapidity of b-jets and of the Z-boson, and for each b-jet, the y_{boost} of the b-jet and Z. For events with $Z\, p_T > 20$ GeV, the $\Delta R, \Delta\phi$, and Δy between the Z and all b-jets are plotted. For events with at least two b-jets, the ΔR and di-b-jet mass for the two leading b-jets, along with the Z p_T and rapidity are plotted.

[1] Contributing authors: M. Bell, J. Butterworth, V. Ciulli, G. Hesketh, F. Krauss, G. Luisoni, G. Nail, D. Napoletano, C. Oleari, S. Platzer, C. Reuschle, B. Waugh, ...

[2] Leptons are dressed by adding the four-vectors of all photons within $\Delta R < 0.1$ to the lepton 4-vector

For this study, further distributions were added: the p_T of all weakly decaying b hadrons with $|y| < 2.7$, and the p_T of the subset of those that are matched to a jet. For b-jets, the number of matching b-hadrons, and the jet p_T for jets with one or two matching b-hadrons are plotted, all with and without the 5 GeV requirement on b-hadron p_T. Finally the ratio of the number of jets matching one to those matching two b-had rons is plotted as a function of jet p_T. All of these additional distributions are also formed using b-quarks instead of b-hadrons.

- Measurement of the cross-section for W boson production in association with b-jets in pp collisions at $\sqrt{s} = 7$ TeV with the ATLAS detector [5] (Rivet routine ATLAS_2013_I1219109). A dressed lepton with $p_T > 25$ GeV and $|\eta| < 2.5$ and a same-flavour neutrino with $p_T > 25$ GeV are used to form a W candidate, which is required to have a transverse mass greater than 60 GeV. Anti-k$_t$ 0.4 jets are reconstructed from all final state particles, and required to have $p_T >$25 GeV, $|y| < 2.1$ and not overlap with the charged lepton used to make the W candidate ($\Delta R(jet, l) > 0.5$). Events with more than two selected jets are vetoed, and the at least one of the selected jets is required to be labelled as b-jet, based on matching with $\Delta R < 0.3$ to a weakly decaying b-hadron with $p_T > 5$ GeV.
  Distributions include the number of b-jets, and the b-jet p_T in events containing exactly one or two selected jets. The same additional distributions for the Z analysis are also added to this analysis.
- Cross-section and angular correlations in Z boson with b-hadrons events at $\sqrt{s} = 7$ TeV [6] (Rivet routine CMS_2013_i1256943). A pair of opposite sign charge dressed lepton with $p_T > 20$ GeV and $|\eta| < 2.4$ are required, with dilepton mass between 81 and 101 GeV. Exactly two weakly decaying b-hadrons with $p_T > 15$ GeV and $|\eta| < 2$ are then required.
  Distributions include the Z p_T, the ΔR and $\Delta\phi$ between b-hadrons, ΔR between the Z and closest b-hadron, and the asymmetry of the ΔR between the Z and closest b-hadron, and the Z and the furthest b-hadron. The angular distributions are repeated with a requirement of Z $p_T > 50$ GeV.

1.3 Event generators

1.31 SHERPA

In this section we present results obtained with the SHERPA event generator [7]. In particular we consider three different classes of samples: 4F MC@NLO, 5F MEPS and a 5F MEPS@NLO one.

4F MC@NLO: This first set of results is obtained in the four-flavour scheme, and based on the MC@NLO technique [2], as implemented in SHERPA [8]. In a four-flavour scheme calculation, b–quarks can only be produced as final state massive particles. They are, therefore, completely decoupled from the evolution of the strong coupling, α_S and that of the PDFs. In this scheme the associated production at tree-level starts from processes such as $jj \to b\bar{b}Z$ where j can be either a light quark or a gluon. No specific cuts are applied on the b–quarks, their finite mass regulates collinear divergences that would appear in the massless case. In most cases, therefore, a b-jet actually originates from the parton shower evolution and hadronization of a b–quark produced by the matrix element.

5F MEPS: In a 5F scheme b–quarks are treated as massless partons. Collinear logs are resummed into a b–PDF and they can appear as initial state particles as well as final state ones. In order to account for 0 and 1 b–jets bins as well as to cure the collinear singularity that would arise with a massless final state parton, we use multi-jet merging. In SHERPA, the well-established mechanism for combining into one inclusive sample towers of matrix elements with increasing jet multiplicity at tree–level is the CKKW [9]. For this sample we merge together LO samples of $jj \to Z$, $jj \to Z + j$, $jj \to Z + jj$, $jj \to Z + jjj$ where now j can be a light quark, a b–quark or a gluon, and all these samples are further matched to the SHERPA parton shower CSS [10]. Merging rests on a jet-criterion, applied to the matrix elements. As a result, jets are being produced by the fixed–order matrix elements and further evolved by the parton shower. As a consequence, the jet criterion separating the two regimes is typically chosen such that the jets produced by the shower are softer than the jets entering the analysis. This is realised here by a cut-off of $\mu_{\rm jet} = 10$ GeV.

5F MEPS@NLO: In this scheme we use the extension to next–to leading order matrix elements, in a technique dubbed MEPS@NLO [11]. In particular, we merge $jj \to Z$, $jj \to Z + j$, $jj \to Z + jj$ calculated with NLO accuracy and we further merge this sample with $jj \to Z + jjj$ at the LO. As in the previous case matching criterion has to be chosen, and this is realised by a cut-off of $\mu_{\text{jet}} = 10$ GeV.

In SHERPA, tree–level cross sections are provided by two matrix element generators, AMEGIC++ [12] and COMIX [13], which also implement the automated infrared subtraction [14] through the Catani–Seymour scheme [15, 16]. For parton showering, the implementation of [10] is employed with the difference that for $g \to b\bar{b}$ splittings the invariant mass of the $b\bar{b}$ pair, instead of their transverse momentum, is being used as scale. NLO matrix elements are instead obtained from OPENLOOPS [17, 18].

1.32 HERWIG7

In this section we present the setup for those results obtained with the HERWIG7 event generator [19, 20].

Based on extensions of the previously developed MATCHBOX module [21], HERWIG7 facilitates the automated setup of all ingredients necessary for a full NLO QCD calculation in the subtraction formalism: an implementation of the Catani–Seymour dipole subtraction method [15, 16], as well as interfaces to a list of external matrix–element providers – either at the level of squared matrix elements, based on extensions of the BLHA standard [22, 23, 24], or at the level of color–ordered subamplitudes, where the color bases are provided by an interface to the COLORFULL [25] and CVOLVER [26] libraries.

For this study the relevant tree–level matrix elements are provided by MADGRAPH_MC@NLO [27, 28] (at the level of color–ordered subamplitudes), whereas the relevant tree–level/one–loop interference terms are provided by OPENLOOPS [17, 18] (at the level of squared matrix elements).

Fully automated NLO matching algorithms are available, henceforth referred to as subtractive (NLO$\oplus$) and multiplicative (NLO$\otimes$) matching – based on the MC@NLO [2] and Powheg [3] formalism respectively – for the systematic and consistent combination of NLO QCD calculations with both shower variants [29, 30] in HERWIG7.

We consider four different classes of samples, for varying combinations of matching and shower algorithms (a selection of plots can be found in sections 1.42 and 1.52):

4F, Zbb For this set we consider the subtractive and multiplicative matching together with the $\tilde{q}$ shower. The core tree–level process in this case is $jj \to Zb\bar{b} \to l^+l^-b\bar{b}$, where $l \in \{e, \mu\}$. For the production runs only $l = e$ is actually considered. In a four–flavour scheme the b quark is typically considered massive and j can only consist of light quarks or a gluon, not a b quark.

5F, Zbb For this set we consider the subtractive and multiplicative matching together with the $\tilde{q}$ and dipole shower. The core tree–level process in this case is $jj \to Zb\bar{b} \to l^+l^-b\bar{b}$, where $l \in \{e, \mu\}$. For the production runs only $l = e$ is actually considered. In a five–flavour scheme the b quark is treated as massless, and j may also include a b quark. Generator–level cuts on the b quarks have thus been applied. Only in the shower evolution of the $\tilde{q}$ shower is the b quark assumed massive.

5F, Zb For this set we consider the subtractive and multiplicative matching together with the $\tilde{q}$ and dipole shower. The core tree–level process in this case is $jj_b \to Zj_b \to l^+l^-j_b$, where $l \in \{e, \mu\}$. For the production runs only $l = e$ is actually considered. In a five–flavour scheme the b quark is treated as massless. For single b–quark production j must not include a b quark, but $j_b \in \{b, \bar{b}\}$. Generator–level cuts on the b quark have thus been applied. Only in the shower evolution of the $\tilde{q}$ shower is the b quark assumed massive.

4F, Wbb For this set we consider the subtractive and multiplicative matching together with the $\tilde{q}$ shower. The core tree–level process in this case is $jj' \to Wb\bar{b} \to l\nu_l b\bar{b}$, where $l \in \{e^+, e^-, \mu^+, \mu^-\}$ and ν_l the associated neutrino. In a four–flavour scheme the b quark is typically considered massive and j, j' can only consist of light quarks or a gluon, not a b quark.

1.33 Powheg

1.4 Z+b(b) production

1.41 Z+b(b) with SHERPA

Figures 1 and 2 show a selection of the plots compairing Sherpa predictions to data. There is overall a good agreement, but for the normalization. The 5F LO order predictions are generally below the data, though compatible within the large scale uncertainty. For NLO predictions this uncertainty is smaller and some patterns can be observed. Both the 5F and the 4F NLO are in good agreement with distributions for events with two b-tagged jets. But when a single b-jet is tagged, the 5F and 4F results have an opposite behaviour: the 5F is 20% above the data (except for high Z p_T), while 4F is 20% below.

It is nevertheless remarkable that the ratio of 4F NLO predictions to data is flat for all the observables. This is particularly interesting, since it is more efficient to generate a sample of $Z + b\bar{b}$ events with the 4F scheme than with the 5F. The reason why an overall normalization factor is needed could lie in the large logarithms, that in the 5F scheme are resummed in the b parton distribution function. However they might not affect the shape of the distributions. To check this hypothesis the 4F NLO predictions have been rescaled to the best available inclusive cross-sections *FIXME:UNCERTAINTY BAND/REFERENCES*. A selection of the plots is shown in Figure 3. The results are very encouraging but further studies are needed to undestand if this approach fails for other observables, e.g. those related to the presence of additional light-quark jets.

1.42 Z+b(b) with HERWIG7

1.5 W+b production

1.51 W+b with Powheg

1.52 W+b with HERWIG7

1.53 W+b with SHERPA

FIXME: SHERPA IS LO/NLO? REMOVE HERWIG FROM THESE PLOTS? ADD ALSO RATE PLOT HERE OR REMOVE EVERYWHERE?

1.6 Conclusions

References

[1] F. Maltoni, G. Ridolfi, and M. Ubiali, *JHEP* **07** (2012) 022, [1203.6393]. [Erratum: JHEP04,095(2013)].

[2] S. Frixione and B. R. Webber, *JHEP* **06** (2002) 029, [hep-ph/0204244].

[3] P. Nason, *JHEP* **11** (2004) 040, [hep-ph/0409146].

[4] G. Aad *et. al.*,, **ATLAS** Collaboration *JHEP* **10** (2014) 141, [1407.3643].

[5] G. Aad *et. al.*,, **ATLAS** Collaboration *JHEP* **06** (2013) 084, [1302.2929].

[6] S. Chatrchyan *et. al.*,, **CMS** Collaboration *JHEP* **12** (2013) 039, [1310.1349].

[7] T. Gleisberg, S. Höche, F. Krauss, M. Schönherr, S. Schumann, F. Siegert, and J. Winter, *JHEP* **02** (2009) 007, [0811.4622].

[8] S. Hoeche, F. Krauss, M. Schonherr, and F. Siegert, *JHEP* **09** (2012) 049, [1111.1220].

[9] S. Catani, F. Krauss, R. Kuhn, and B. R. Webber, *JHEP* **11** (2001) 063, [hep-ph/0109231].

[10] S. Schumann and F. Krauss, *JHEP* **03** (2008) 038, [0709.1027].

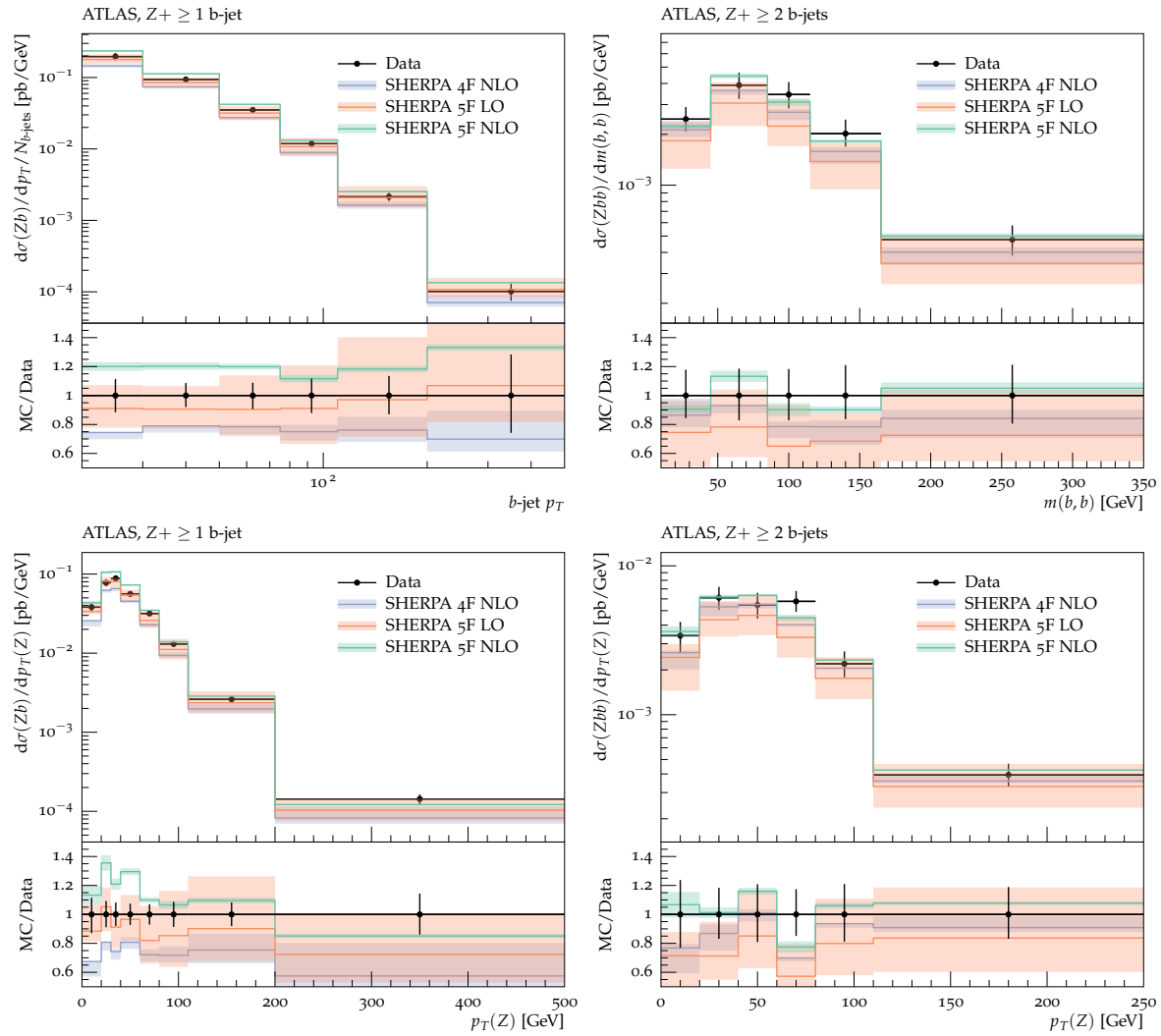

Fig. 1: A selection of the plots compairing Sherpa predictions to ATLAS results.

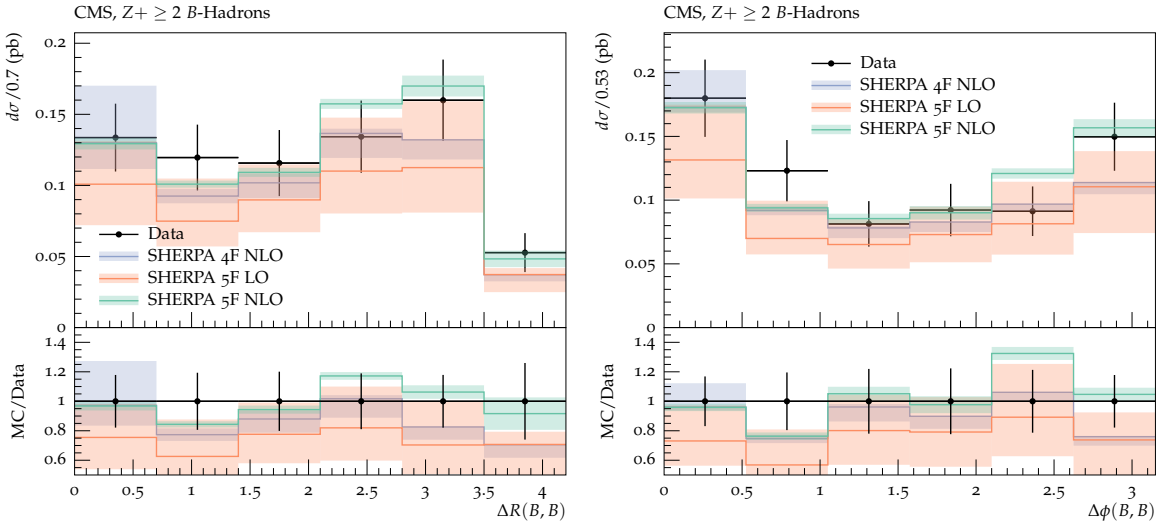

Fig. 2: A selection of the plots compairing Sherpa predictions to CMS results.

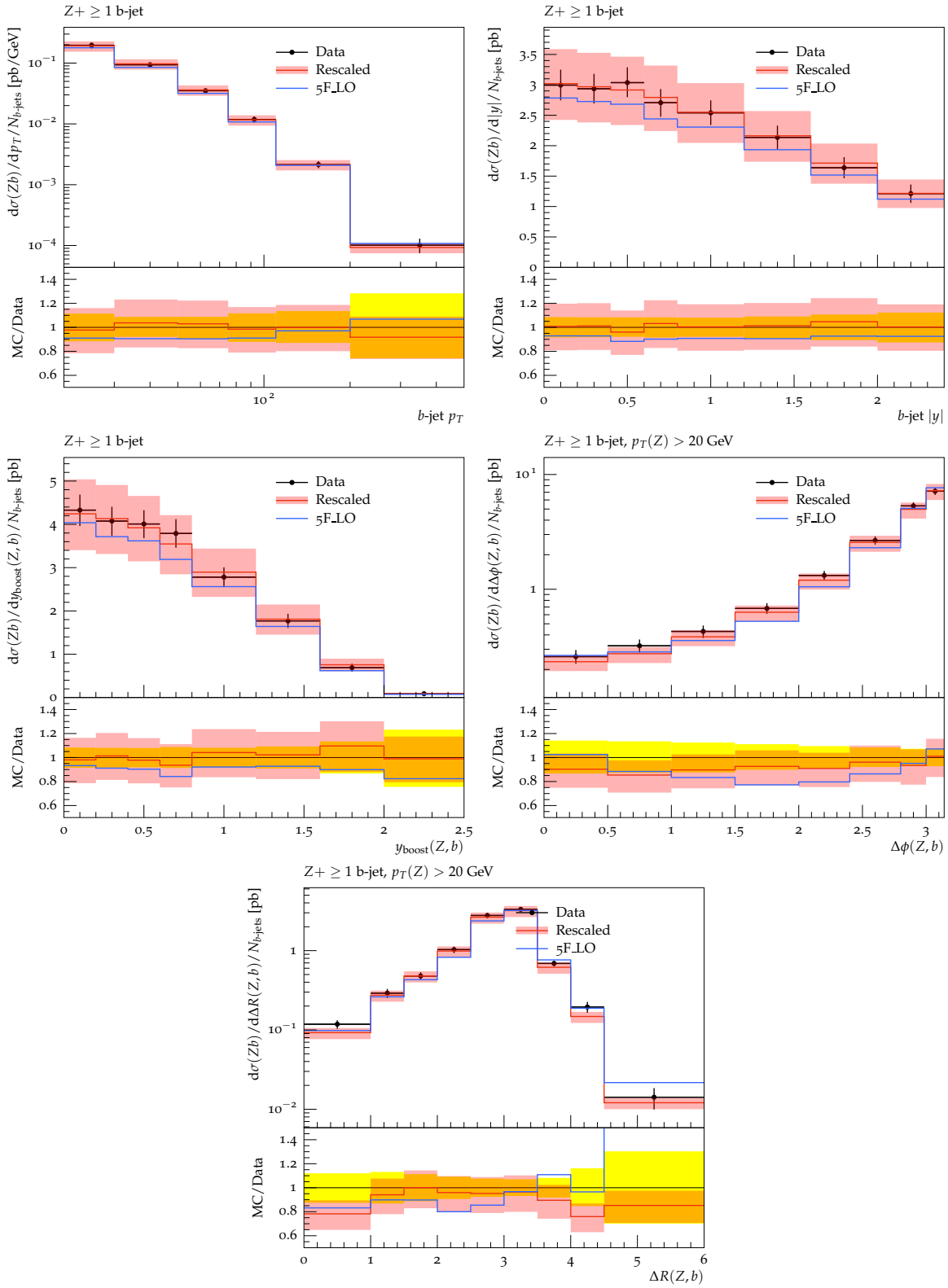

Fig. 3: *FIXME:REMOVE ONE PLOT OR ADD Z PT?* A selection of the plots compairing rescaled Sherpa 4F NLO predictions to ATLAS results.

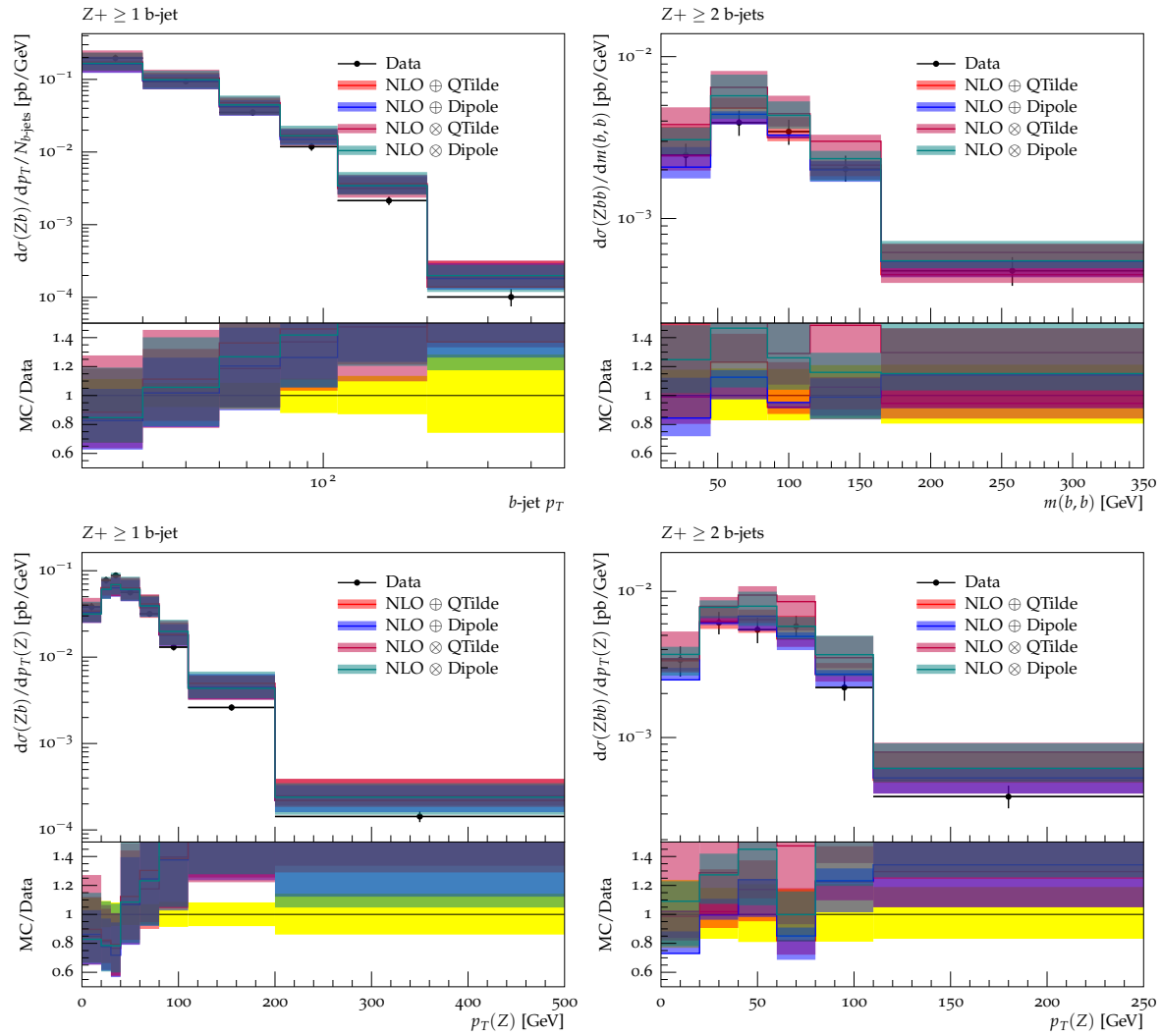

Fig. 4: A selection of the plots compairing Herwig 5F Zbb predictions to ATLAS results.

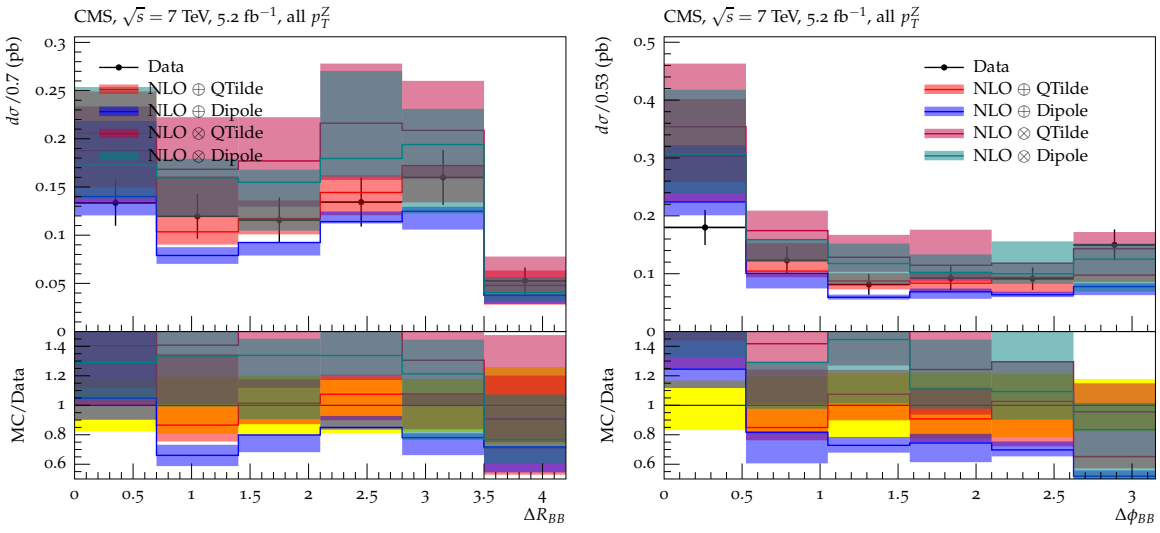

Fig. 5: A selection of the plots compairing Herwig 5F Zbb predictions to CMS results.

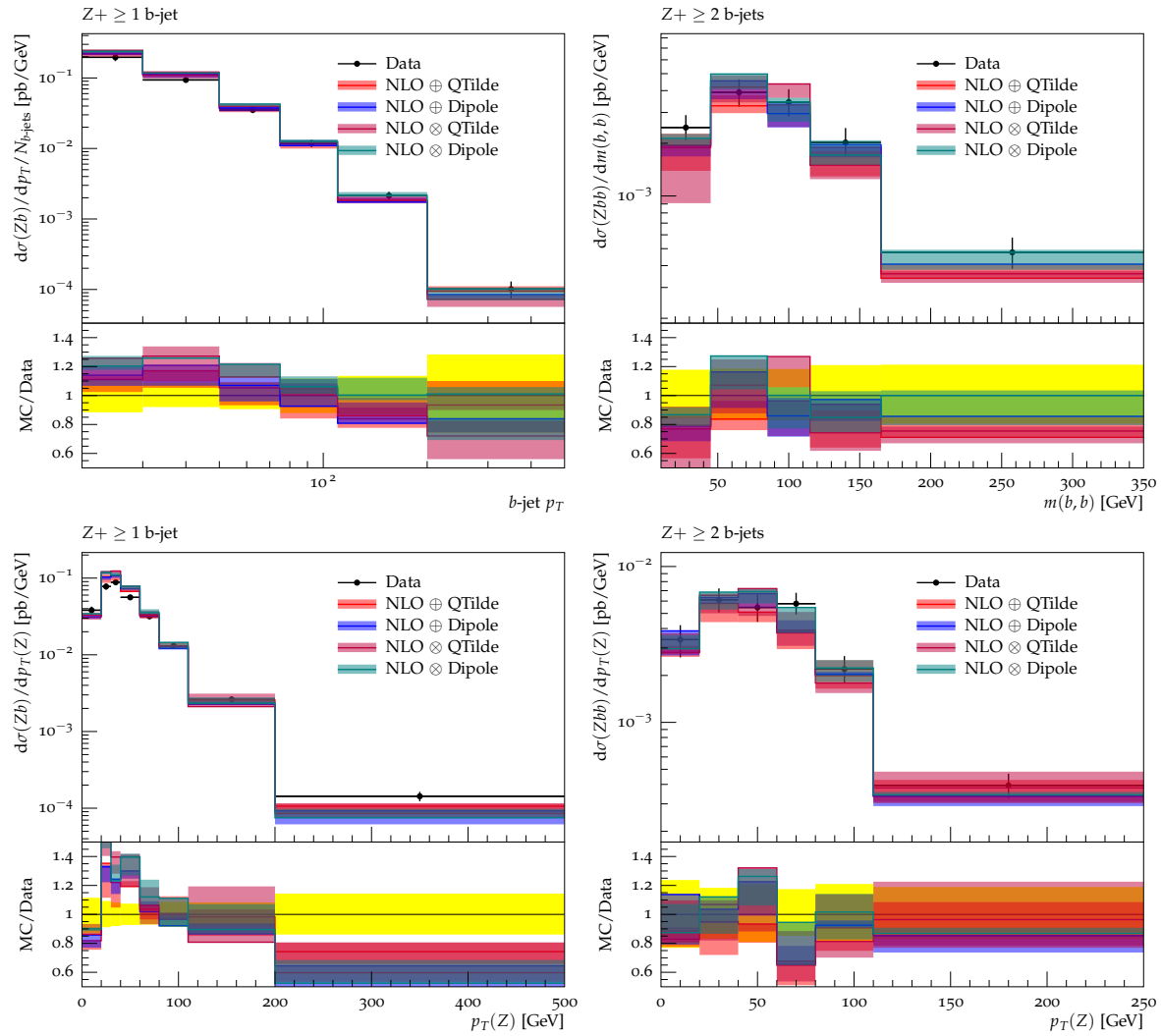

Fig. 6: A selection of the plots compairing Herwig 5F Zb predictions to ATLAS results.

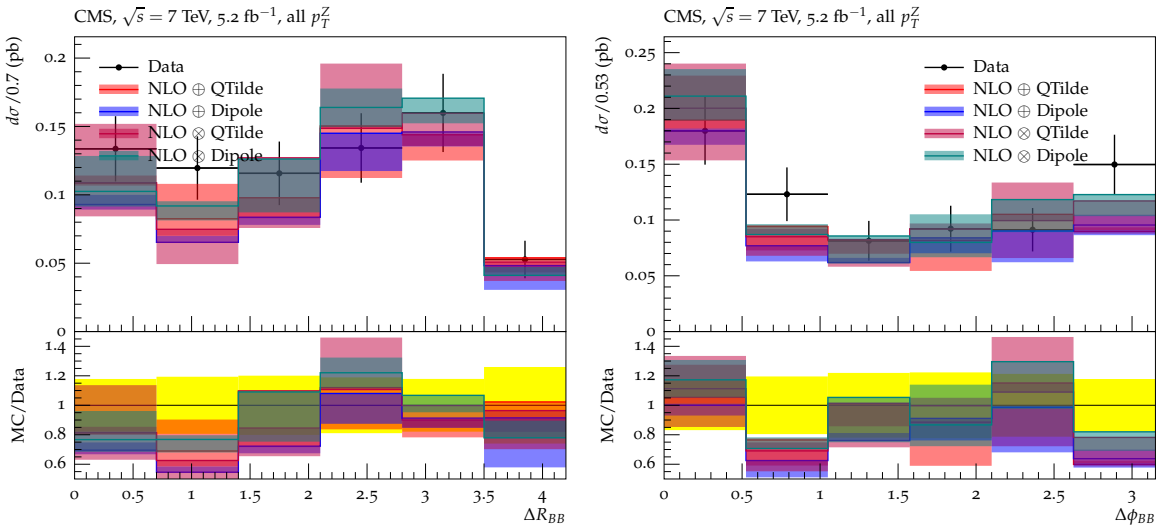

Fig. 7: A selection of the plots compairing Herwig 4F Zbb predictions to CMS results.

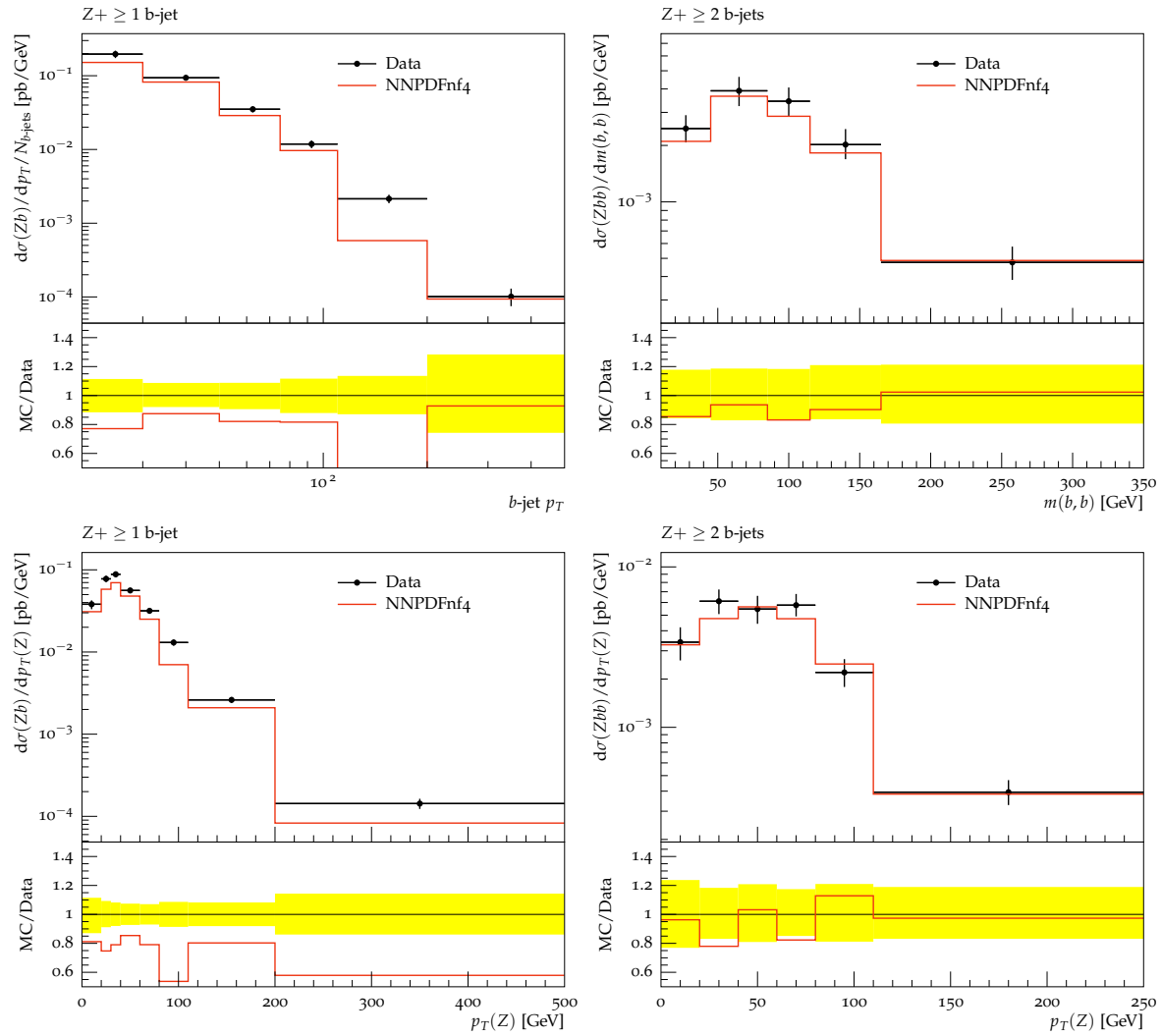

Fig. 8: A selection of the plots compairing Herwig 4F Zbb predictions to ATLAS results.

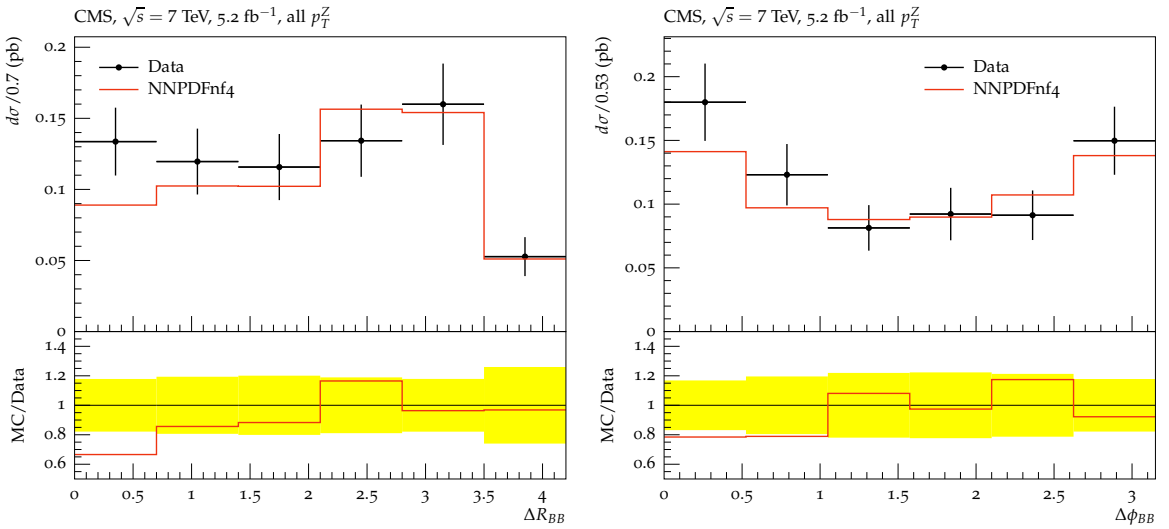

Fig. 9: A selection of the plots compairing Herwig 4F Zbb predictions to CMS results.

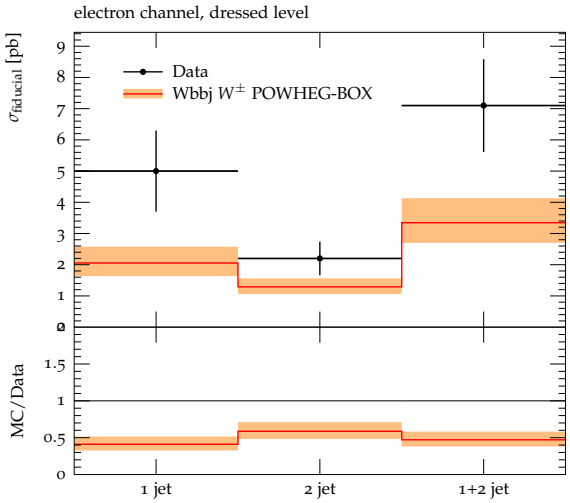

Fig. 10: Cross-section for $W + b$ events with at least one b-jet vs the total number of jets in the event. Superimposed are shown the predictions from Powheg $W + b\bar{b}j$ NLO.

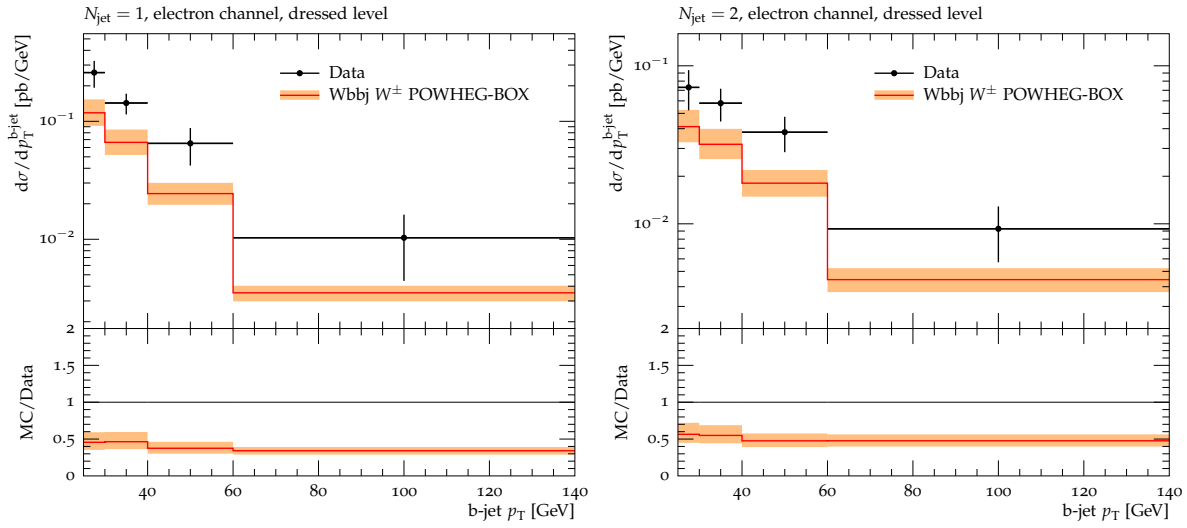

Fig. 11: Differential p_T distribution of the b-jet in $W + b$ events with a single jet (left) or with two jets (right). Superimposed are shown the predictions from Powheg $W + b\bar{b}j$ NLO.

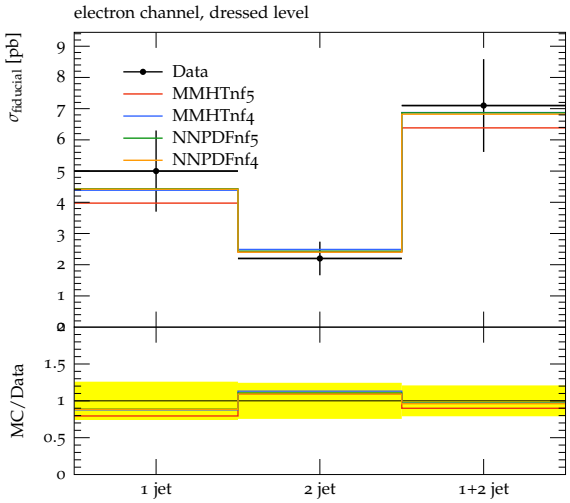

Fig. 12: Cross-section for $W + b$ events with at least one b-jet vs the total number of jets in the event. Superimposed are shown the predictions from Herwig $W + b\bar{b}$ NLO.

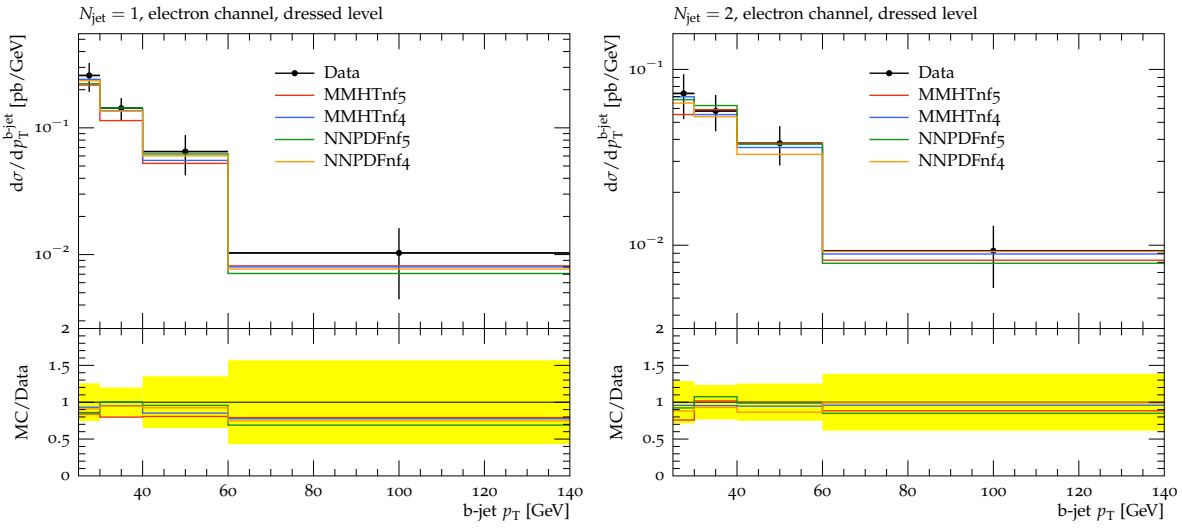

Fig. 13: Differential p_T distribution of the b-jet in $W + b$ events with a single jet (left) or with two jets (right). Superimposed are shown the predictions from Herwig $W + b\bar{b}$ NLO.

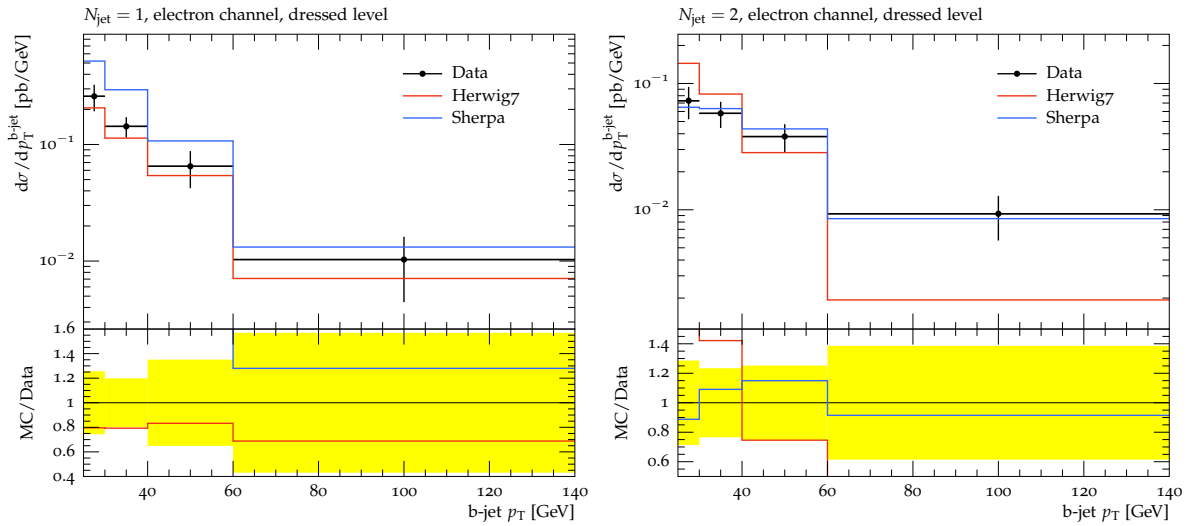

Fig. 14: Differential p_T distribution of the b-jet in $W + b$ events with a single jet (left) or with two jets (right). Superimposed are shown the predictions from Sherpa $W + b\bar{b}j$

[11] S. Hoeche, F. Krauss, M. Schonherr, and F. Siegert, *JHEP* **1304** (2013) 027, [1207.5030].

[12] F. Krauss, R. Kuhn, and G. Soff, *JHEP* **02** (2002) 044, [hep-ph/0109036].

[13] T. Gleisberg and S. Höche, *JHEP* **12** (2008) 039, [0808.3674].

[14] T. Gleisberg and F. Krauss, *Eur. Phys. J.* **C53** (2008) 501–523, [0709.2881].

[15] S. Catani and M. H. Seymour, *Nucl. Phys.* **B485** (1997) 291–419, [hep-ph/9605323].

[16] S. Catani, S. Dittmaier, M. H. Seymour, and Z. Trocsanyi, *Nucl. Phys.* **B627** (2002) 189–265, [hep-ph/0201036].

[17] F. Cascioli, P. Maierhofer, and S. Pozzorini, *Phys. Rev. Lett.* **108** (2012) 111601, [1111.5206].

[18] F. Cascioli, S. Hche, F. Krauss, P. Maierhfer, S. Pozzorini, and F. Siegert, *J. Phys. Conf. Ser.* **523** (2014) 012058.

[19] J. Bellm *et. al.*, 1512.01178.

[20] M. Bahr *et. al.*, *Eur. Phys. J.* **C58** (2008) 639–707, [0803.0883].

[21] S. Platzer and S. Gieseke, *Eur. Phys. J.* **C72** (2012) 2187, [1109.6256].

[22] T. Binoth *et. al.*, *Comput. Phys. Commun.* **181** (2010) 1612–1622, [1001.1307]. [,1(2010)].

[23] S. Alioli *et. al.*, *Comput. Phys. Commun.* **185** (2014) 560–571, [1308.3462].

[24] J. R. Andersen *et. al.*, 1405.1067.

[25] M. Sjodahl, *Eur. Phys. J.* **C75** (2015), no. 5 236, [1412.3967].

[26] S. Pltzer, *Eur. Phys. J.* **C74** (2014), no. 6 2907, [1312.2448].

[27] J. Alwall, M. Herquet, F. Maltoni, O. Mattelaer, and T. Stelzer, *JHEP* **06** (2011) 128, [1106.0522].

[28] J. Alwall, R. Frederix, S. Frixione, V. Hirschi, F. Maltoni, O. Mattelaer, H. S. Shao, T. Stelzer, P. Torrielli, and M. Zaro, *JHEP* **07** (2014) 079, [1405.0301].

[29] S. Gieseke, P. Stephens, and B. Webber, *JHEP* **12** (2003) 045, [hep-ph/0310083].

[30] S. Platzer and S. Gieseke, *JHEP* **01** (2011) 024, [0909.5593].